



Gjøvik University College

HiGIA

Gjøvik University College Institutional Archive

*Cheffena, M., Fontán, F. P., Lacoste, F., Corbel, E., Mametsa, H.-J. & Carrie, G. (2012).
Land Mobile Satellite Dual Polarized MIMO Channel Along Roadside Trees:
Modeling and Performance Evaluation. IEEE Transactions on Antennas and
Propagation, 60 (2): 597-605.*

DOI: 10.1109/TAP.2011.2173447

Please notice:

*This is the author's post-print version of the article published in
IEEE Transactions on Antennas and Propagation
The article has been peer-reviewed,
but does not include the publisher's layout and page numbers.*

© Reprinted with permission from

2012 IEEE. Personal use of this material is permitted. Permission from IEEE must be obtained for all other users, including reprinting/ republishing this material for advertising or promotional purposes, creating new collective works for resale or redistribution to servers or lists, or reuse of any copyrighted components of this work in other works

Land Mobile Satellite Dual Polarized MIMO Channel along Roadside Trees: Modeling and Performance Evaluation

Michael Cheffena, Fernando Perez Fontan, Frederic Lacoste, Erwan Corbel, Henri-Jose Mametsa and Guillaume Carrie

Abstract—We present a novel physical-statistical, generative model for the land mobile satellite (LMS), dual polarized, multiple-input-multiple-output (MIMO) channel along tree sided roads. Said model is parameterized by means of a physical model based on the Multiple Scattering Theory (MST) which accounts for the signal attenuation and scattering by trees. Moreover, Finite-Difference Time-Domain (FDTD) electromagnetic computations were performed to characterize the scattering pattern of an isolated tree, and to calculate the MIMO shadowing correlation matrix required by the model, and not provided by MST. This modeling framework also encompasses the single-input-multiple-output (SIMO)/space diversity case. To illustrate the capabilities of the developed model, time series were generated and used in system performance calculations. The obtained results give an insight into the advantages of dual polarized MIMO and SIMO/space diversity techniques in these very frequent scenarios, and may help service providers in evaluating the technical feasibility of such systems.

Index Terms—LMS MIMO, diversity, signal fading, vegetation.

I. INTRODUCTION

THE true broadcast nature of satellite-based mobile communication systems offers great advantages for delivering multicast and broadcast services to both populated and isolated areas. However, due to the high path loss, limited satellite power, and other impairments, current land mobile satellite (LMS) systems show lower capacities and availabilities than those of terrestrial systems [1]. Their performance can be increased using multiple-input-multiple-output (MIMO) techniques. To design such systems, a good understanding of the propagation channel is required.

Signal propagation in the LMS channel is affected by different propagation impairments, among which are signal

attenuation and fading caused by vegetation. The signal attenuation due to vegetation depends on a range of factors such as tree type, whether the trees are in-leaf or out-of-leaf, whether the trees are dry or wet, the frequency band, the path length through foliage, etc. [2]. A single-input-single-output (SISO), roadside tree LMS channel model which takes into account the signal fading caused by position-dependent tree scattered fields and by swaying tree components due to wind was reported in [3] and [4]. Fade mitigation techniques (FMTs) such as MIMO might be used to counteract the signal fading caused by vegetation. Availability of realistic channel time series and detailed knowledge of their correlation properties are needed for performing accurate simulations [5]. Several studies on terrestrial MIMO systems can be found in the literature, while studies on LMS MIMO are rather limited, among them are [1], [6]–[9].

In this paper, we present a novel physical-statistical, generative channel model for the roadside tree, LMS, dual polarized MIMO channel which includes as a special case the single-input-multiple-output (SIMO) case. Figure 1 shows the considered propagation scenario where a mobile terminal receives partially correlated co- and cross-polar, right and left hand circular polarized (R/LHCP) tree scattered fields from both sides of the road. The wanted model requires parameterization; this is achieved by means of a physical model based on the Multiple Scattering Theory (MST) [10]–[12]. This technique is used to estimate the signal attenuation and scattering by a single tree. MST assumes a uniform distribution of scatterers in both azimuth $[0, 2\pi)$ and elevation $(0, \pi/2)$ [3], [4], [13]. This assumption makes it impossible to quantify spatial effects such as the cross-correlation of the shadowing affecting the direct signal reaching the receive antennas. To overcome this, Finite-Difference Time-Domain (FDTD) electromagnetic computations were performed to accurately calculate the MIMO shadowing correlation matrix. In addition, calculated tree scattering patterns are also shown which coincide with results obtained using MST.

To show the potential of the proposed physical-statistical, generative model, examples of performance evaluation for SISO, SIMO and MIMO configurations were carried out using synthesized time series. The results give an insight into the advantages of polarization MIMO and SIMO/space diversity techniques, and may be used in assessing the technical feasibility of LMS systems in roadside tree scenarios.

The paper begins in Section II by presenting the FDTD

This work is supported by the French Space Agency (CNES), French Aerospace Lab (ONERA) and Thales Alenia Space - France.

M. Cheffena is with Gjøvik University College, Teknologivn. 22, N-2815 Gjøvik, Norway (e-mail: Michael.Cheffena@hig.no).

F. Perez Fontan is with the University of Vigo, E-36200 Vigo, Spain (e-mail: ffontan@tsc.uvigo.es).

F. Lacoste is with CNES, 18 avenue Edouard Belin, F-31401 Toulouse, France (e-mail: Frederic.Lacoste@cnes.fr).

E. Corbel is with Thales Alenia Space - France, 26 avenue J. F. Champollion, F-31037 Toulouse, France (e-mail: Erwan.Corbel@thalesaleniaspace.com).

H. Mametsa is with ONERA, 2 avenue Edouard Belin, F-31055 Toulouse, France (e-mail: Henri-Jose.Mametsa@onera.fr).

G. Carrie is with ONERA, 2 avenue Edouard Belin, F-31055 Toulouse, France (e-mail: Guillaume.Carrie@onera.fr).

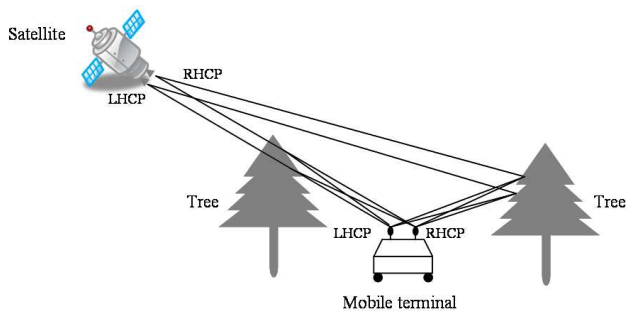


Fig. 1. Propagation scenario for the LMS dual polarized MIMO: a mobile terminal receives correlated co- and cross-polar (R/LHCP) tree attenuated and scattered fields from both sides of the road.

electromagnetic computation results. Section III discusses the basis of the proposed physical-statistical model which, in general, is oriented toward a MIMO configuration but also encompasses both the SISO and SIMO configurations. In this section the MST based SISO channel model used for parameterizing direct signal attenuation and multipath is briefly discussed. Then we discuss the SIMO case. Finally, we go on to present the dual polarized, physical-statistical, generative MIMO channel model. In Section IV we present examples performance calculations using synthetic time series. Such calculations include capacity and diversity studies. Finally, the conclusions are given in Section V.

II. FDTD COMPUTATION

FDTD, Finite-Difference Time-Domain, is a numerical technique for solving electromagnetic problems where the computation space is divided into small cubic cells in which the time-domain fields are solved using an explicit finite-difference update scheme. Using FDTD, accurate solutions of the electromagnetic interaction with arbitrary-shaped objects can be obtained [14]. In this section, the attenuation and scattering characteristics of a tree are computed using an FDTD tool. The attenuation time series are further used to extract the correlation matrix of the shadowing effects in the LMS dual polarized MIMO channel of interest.

The input to FDTD is a three dimensional cubically meshed tree model having a dielectric constant of 28 [13] and conductivity of 0.02 S/m [15]. The dimensions of the tree in the x , y , and z directions are 2.74 m, 2.64 m, and 3.17 m, respectively. The FDTD computation space and the tree model used are shown in Fig. 2. The computational volume is divided into a scattering field region and a total field region (which also includes the incident wave) by a virtual plane on which a plane wave is incident into the total field region. The whole region is surrounded by a perfectly matched layer (PML) implementing the absorbing boundary conditions needed to prevent false echoes from being produced at the boundaries of the computational volume. A cell size of 1 cm was utilized which resulted in a highest usable frequency of 3 GHz. The number of cells in the x , y , and z directions were 373, 363, and 417, respectively, which resulted in a total of 56,461,383 cells.

TABLE I
MIMO SHADOWING CORRELATION COEFFICIENTS OBTAINED FROM FDTD SIMULATIONS

	R/R	L/L	R/L	L/R
R/R	1	0.87	0.30	0.43
L/L	0.87	1	0.26	0.47
R/L	0.30	0.26	1	0.49
L/R	0.43	0.47	0.49	1

Two scenarios were investigated: the far-field scattering pattern and the total field in a straight line along the y -axis behind the tree (see the dashed line in Fig. 2). Two runs of the FDTD tool were performed, one with a vertical and the other with a horizontal polarized incident wave. These were then combined to yield circularly polarized signals. A Gaussian pulse was used as the source field. A near-to-far-field transformation was performed to calculate the far-field scattering pattern.

Figs. 3 and 4 show the normalized far-field scattering pattern of the co- and cross-polar components of the RHCP and LHCP signals at 2 GHz, respectively. The results are obtained by rotating the observation point 360° around the tree as shown in Fig. 2, where zero deg. represents the line-of-sight (LOS) path between the satellite and the mobile terminal (through the tree). We can observe that the scattering patterns of the co-polar components have a forward lobe with an isotropic background, the same as with MST, as reported in [3] and [4], or the Radiative Energy Transfer, RET, as reported in [16]. Fig. 5 shows the total received field along a straight line parallel to the y -axis behind the tree for the co- and cross-polar components of the RHCP and LHCP signals. The points at the start (before 0 m) and at the end of the straight line (after 2.64 m) are not blocked (LOS conditions) toward the source while the rest are shadowed by the tree (the tree is located between 0 to 2.64 m along y -axis). The fields along the straight line are passed through a running average filter (with ten point window size) for calculating the large-scale fading (shadowing) effects caused by the tree, see Fig. 6.

As we move along the positive y -axis direction, we can observe from Fig. 6 the change of state due to tree shadowing i.e., LOS-shadowing-LOS. Table I shows the MIMO shadowing (large scale fading) correlation matrix, \mathbf{R}_l , calculated using the mentioned filtered FDTD series at 2 GHz. In Table I, R/R refers to the co-polar signal from a RHCP transmit antenna to a RHCP receive antenna, R/L refers to the cross-polar signal from a RHCP transmit antenna to a LHCP receive antenna, and so on.

Note that the FDTD results presented in this section are only applicable when the tree is in leaf. There exist many very different tree configurations and the shadowing cross-correlation may vary dramatically from tree to tree. This is an issue which requires further investigation, to be carried out at a later time, the main aim of this paper being the description of the physical-statistical model discussed next and how such model can be parameterized.

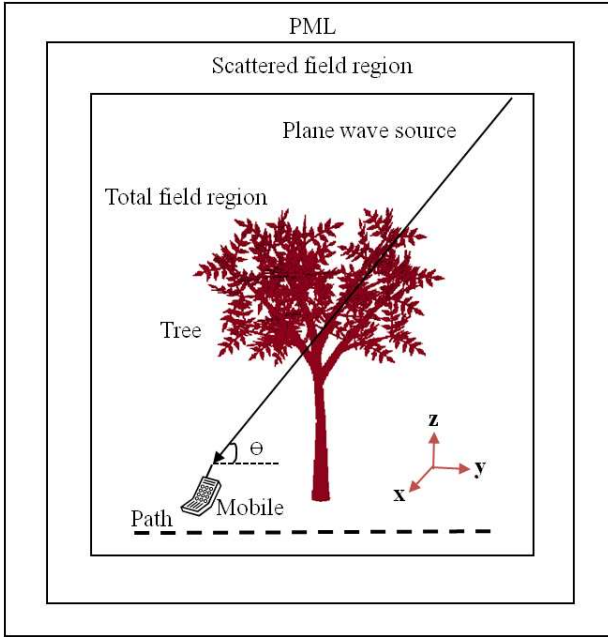


Fig. 2. FDTD computation zones and boundary conditions. Cell size of 1 cm and total cells of 56461383 are used.

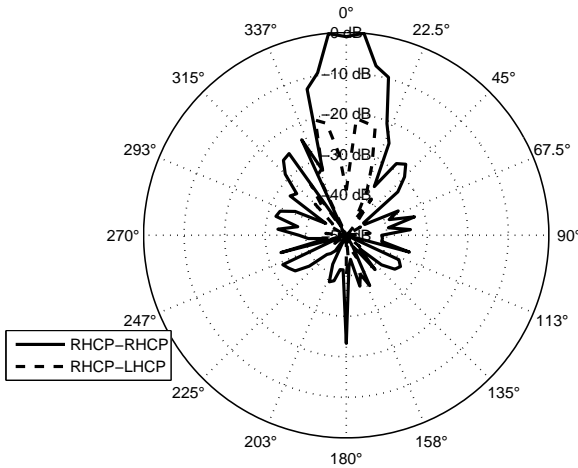


Fig. 3. Scattering patterns of the co- and cross-polar components of the RHCP signal at 2 GHz.

III. PHYSICAL-STATISTICAL, GENERATIVE ROADSIDE TREE LMS DUAL POLARIZED MIMO CHANNEL MODEL

Here a family of physical-statistical, generative models for LMS roadside tree environments is presented, starting with the SISO model and going on to present the SIMO and, finally the MIMO models.

Physical-statistical models are deemed more accurate than purely statistical ones as they take into account the geometry of the link(s), while they rely on physical (electromagnetic-based) methods for calculating the needed model parameters. The underlying assumption made in this family of models is that the received signal is composed of the direct component which may be subjected to shadowing and accompanied by so-called coherent component fluctuations, and the multipath

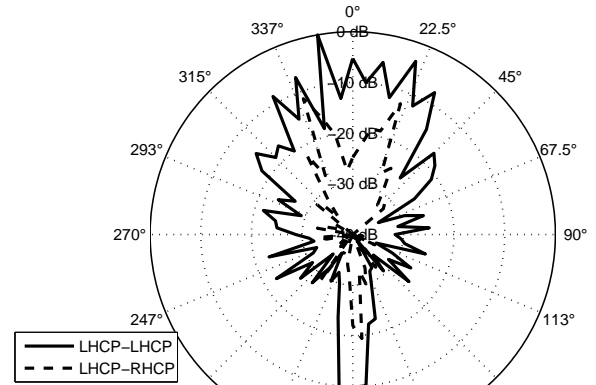


Fig. 4. Scattering patterns of the co- and cross-polar components of the LHCP signal at 2 GHz.

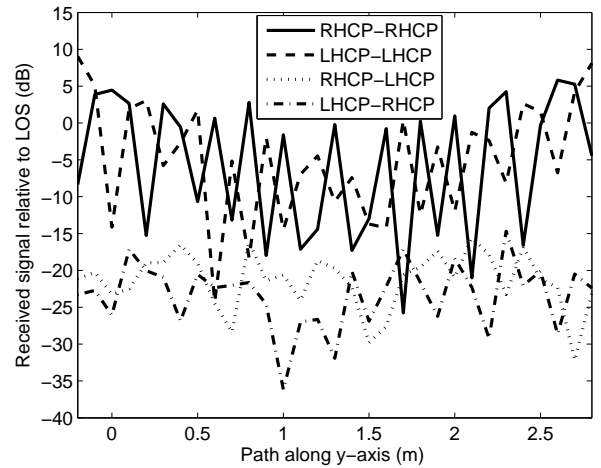


Fig. 5. Time series of the co- and cross-polar components of the RHCP and LHCP signal at 2 GHz.

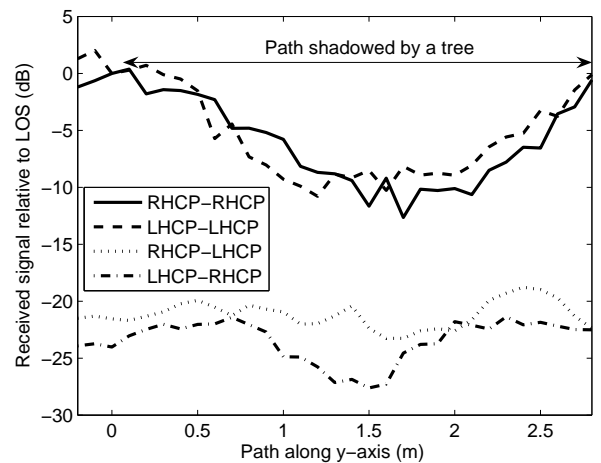


Fig. 6. Shadowing time series of the co- and cross-polar components of the RHCP and LHCP signal at 2 GHz.

component due to diffuse scattering, i.e., a Ricean channel.

Thus we implement a statistical random number generator fitting a Rice distribution whose parameters are changing as the terminal travels through a propagation environment described in terms of simple, canonical volumetric forms representing trees. Also time variations are taken into account, as mentioned earlier, especially for stationary terminals.

The two Rice distribution parameters (direct signal amplitude and multipath power) are calculated using MST: the direct signal is affected by the specific attenuation of the tree canopy provided by MST once the geometrical path through the canopy is worked out for the different terminal route positions. The second component, the multipath power, is also parameterized by means of MST which provides the average coherent and incoherent scattered powers, these are mapped to the relevant Rice distribution parameter, also taking into account the possible paths through and off the tree canopies on both sides of the street.

At least two alternatives are possible for generating locally Ricean time series: one is using a point-scatterer approach (used in the current SISO and SIMO implementations) and the other is by filtering complex random Gaussian series. The latter option has been selected for implementing the MIMO channel.

A. LMS SISO channel model

A SISO model/simulator was reported by the authors in [3] and [4]. The model uses MST as described in [10]–[13] with modifications to account for slant paths and circular polarization. In the model, the tree canopy is modeled as a vertically oriented cylindrical volume, V , in a rectangular coordinate system defined by the orthonormal vectors, \mathbf{x} , \mathbf{y} and \mathbf{z} . The canopy volume contains randomly distributed and oriented leaves and branches. Leaves are modeled as thin lossy dielectric disks, branches as finite lossy dielectric cylinders and the trunk as a finite lossy dielectric cylinder, see Fig. 7.

The SISO model generates the position-dependent signal fading by calculating the total coherent (the sum of coherently scattered and free-space field) and incoherent tree scattered fields. The phase variations in the scattered signal are accounted for using a point-scatterer approach, where the contribution from each tree is assumed to originate from a point in the center of the canopy from which the distance dependent phase variations for the various route sampling points are calculated.

In addition, the signal fading due to wind swaying is accounted for by modeling the tree components as masses attached to springs. The position-dependent fading and the signal fading due to tree swaying are then combined to give the overall signal fading caused by vegetation. The model is applicable for different polarizations and elevation angles, and was validated in terms of first and second order statistics using measurements at 2 GHz, see [3] and [4] for more details.

B. SIMO receiver space diversity

The previously described SISO channel model can easily be extended to the SIMO/space diversity case. The model is

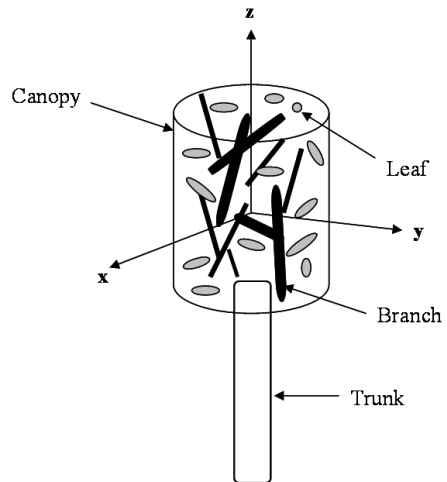


Fig. 7. Tree model for the LMS channel with randomly distributed and oriented leaves and branches. \mathbf{x} , \mathbf{y} and \mathbf{z} are the orthonormal vectors of rectangular coordinate system.

again based on the physical-statistical tree model (see Fig. 7) reported in [3] and [4] and MST. The considered propagation scenario is shown in Fig. 8: two antennas with the same polarization separated by a given distance are receiving tree attenuated and scattered co-polar signals from each side of the road. The fades at each antenna element, $h_{\text{total}}(t)$, are generated by taking into account the tree scattered fields from each side of the road as well as the LOS field, given by

$$h_{\text{side1}}(t) = \sum_{m=1}^{S_1} \sum_{n=1}^N A_{\text{diff1},mn}(t) \frac{\exp\{j(\phi_{mn} + kd_{mn}(t))\}}{d_{mn}(t)} + A_{\text{coh1},m}(t) \frac{\exp\{j(\phi_m + kd_m(t))\}}{d_m(t)} + A_{\text{LOS},m}(t) \frac{\exp\{j(\phi_m + kd_m(t))\}}{d_m(t)} \quad (1)$$

$$h_{\text{side2}}(t) = \sum_{w=1}^{S_2} \sum_{n=1}^N A_{\text{diff2},mn}(t) \frac{\exp\{j(\phi_{wn} + kd_{wn}(t))\}}{d_{wn}(t)} \quad (2)$$

$$h_{\text{total}}(t) = h_{\text{side1}}(t) + h_{\text{side2}}(t) \quad (3)$$

where S_1 and S_2 are the number of trees on each side of the road, N is the total number of scatterers in a single tree and k is the wavenumber. Note here how the overall scattered signal from one single tree has now been split into N components, provided that the link budget of the scattered power and the MST constraints are preserved. This shows a possible way toward a wideband model. Parameters $A_{\text{diff1}}(t)$ and $A_{\text{diff2}}(t)$ are the amplitudes of the incoherent scattered components from side one (satellite side) and side two (opposite side) of the road, respectively. Parameters $A_{\text{coh1}}(t)$ and $A_{\text{LOS}}(t)$ are the amplitudes of the coherent scattered field (side one) and the LOS field, respectively. The coherent and incoherent scattered fields can be estimated from the physical-statistical tree model reported in [3] and [4]. Parameters ϕ and $d(t)$ are the initial phase and path length of each signal component, respectively.

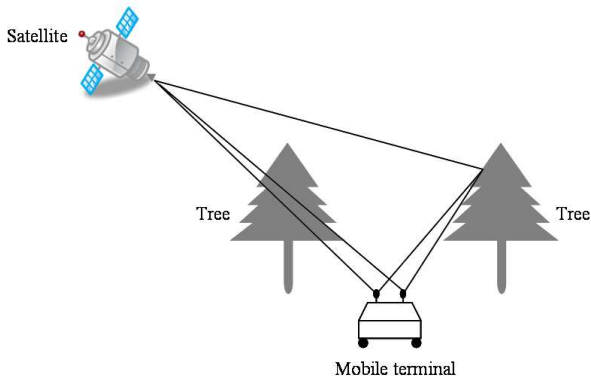


Fig. 8. Roadside tree LMS, SIMO/space diversity propagation scenario: two antennas with the same polarization separated by a given distance are receiving the tree attenuated and scattered co-polar signal from both sides of the road.

The coherent and incoherent scattered fields as well as the LOS field are received from one side of the road, see (1), while only the incoherent scattered fields are received from the other side of the road, see (2). These are combined to produce the signal received at each antenna position, see (3) and Fig. 8.

The resulting simulated correlation coefficient versus antenna separation distance for the small scale fading (absolute values) is shown in Fig. 9 (for two co-polar RHCP antennas). As expected, we can observe that the correlation coefficient decreases with increasing antenna separation distance. The resulting simulated correlation coefficient was also fitted to the square of the zero order Bessel function of the first kind, $(J_0(2\pi d/\lambda))^2$ where d is the relative separation distance and λ is the wavelength, see the dashed line in Fig. 9. It can be seen that the fit between the two curves is quite good. Thus, a model based on the zero-th order Bessel function of the first kind could be used to model the correlation coefficient of the small scale fading in roadside tree LMS SIMO/space diversity channel. Fig. 10 shows examples of simulated received signal time series on the two antennas (RHCP co-polar antennas) for a separation distance of one wavelength. It can be seen that the time series have similar large scale fading characteristics but relatively decorrelated small scale fading due to the separation distance between the two antennas.

C. LMS dual polarized MIMO channel model

The SISO channel model discussed in Section III-A can be extended to the MIMO case by taking into account the correlation between the co- and cross-polar channels. Table I gives the MIMO correlation matrix for the large scale fading obtained using FDTD. The correlation matrix for the small scale fading (multipath), \mathbf{R}_s , can be found by assuming independent multipath fading on the MIMO channels as reported in [1] and [17]. As previously indicated, the underlying assumption is a set of locally Ricean processes whose parameters are slowly-variant along the traveled route. The slow fading correlation properties are then imposed on the direct signal component of the Rice process and the fast variation correlation properties are imposed on the multipath component.

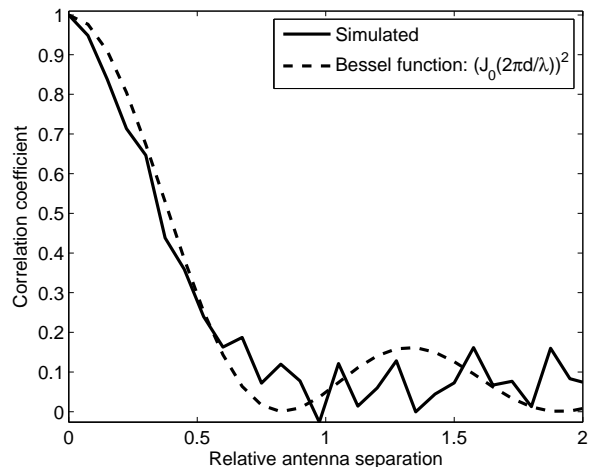


Fig. 9. Small scale fading (absolute values) correlation coefficient versus antenna separation distance (for two co-polar RHCP antennas) for the simulated roadside tree LMS SIMO/space diversity (solid line) channel. Also shown is the theoretical curve of the square of the zero-th order Bessel function of the first kind (dashed line).

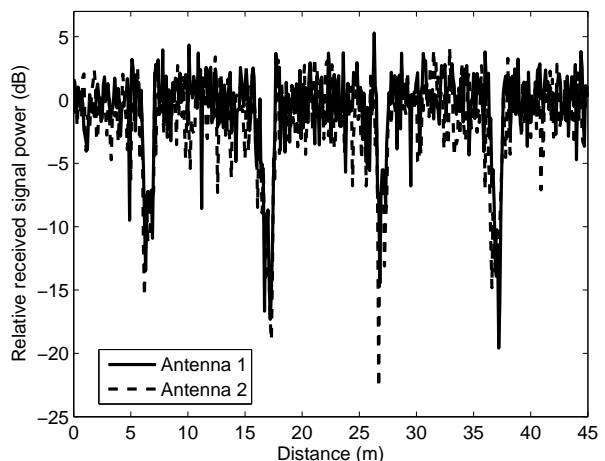


Fig. 10. LMS SIMO receiver space diversity links at antenna separation distance of one wavelength (for two co-polar RHCP antennas).

The proposed model for the roadside tree LMS dual polarized MIMO channel is presented in Fig. 11. In the model, the correlated processes which are the inputs to the shadowing filter (see Fig. 11) are given by

$$\mathbf{l}(t) = \mathbf{C}_l \mathbf{n}_l(t) \quad (4)$$

where $\mathbf{l}(t) = [l_1(t) \dots l_4(t)]^T$ are partially correlated processes. $\mathbf{n}_l(t) = [n_{l1}(t) \dots n_{l4}(t)]^T$ are independent real-valued white Gaussian processes with zero mean and unit variance. \mathbf{C}_l is the Cholesky decomposition of \mathbf{R}_l .

The complex white Gaussian processes, $n_{si}(t)$, (for $i = 1 \dots 4$) are filtered (according to [18]) for Doppler spectrum shaping ($H_{di}(z)$ is the Doppler filter), see Fig. 11. The resulting time series are then multiplied by the standard deviation of the non-coherent component of each channel, $\sigma_i(t)$ (estimated by means of MST [3] and [4]), to produce the small scale fading. Similarly, the partially correlated processes, $l_i(t)$, are

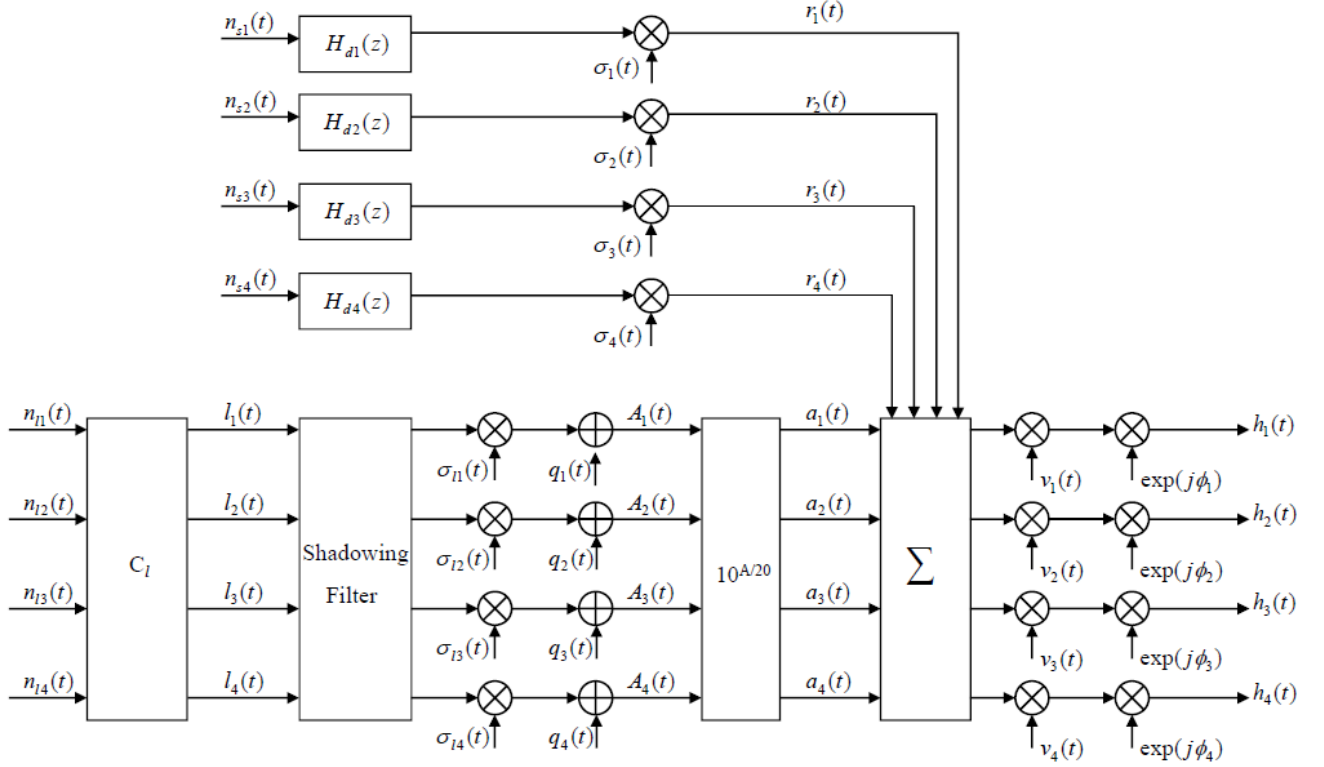


Fig. 11. LMS dual polarized MIMO channel simulator for roadside trees. $n_{s_i}(t)$ and $n_{i_i}(t)$ (for $i = 1 \dots 4$) are independent complex and real-valued white Gaussian processes with zero mean and unit variance, respectively. $H_{d_i}(z)$ is the Doppler filter. C_l is the Cholesky factorization of \mathbf{R}_l . $l_i(t)$ are partially correlated processes. $\sigma_i(t)$ and $q_i(t)$ are the standard deviation of the incoherent and the mean total coherent (which is the sum of coherently scattered and free-space field) component, respectively. $\sigma_{l_i}(t)$ is the standard deviation of the total coherent component. $r_i(t)$ and $a_i(t)$ are the small and large scale fading, respectively. $v_i(t)$ is the fading due to swaying vegetation. ϕ_i is the signal phase corresponding to the traveled distance. $\exp(j\phi_i)$ is the Doppler shift of the direct signal component. $h_i(t)$ is a correlated complex signal envelope of the LMS dual polarized MIMO channel.

low-pass filtered by a shadowing filter with transfer function given by [19]

$$H_s(z) = \frac{\sqrt{1-b^2}}{1-bz^{-1}} \quad (5)$$

with

$$b = \exp\left(-\frac{d_{st}}{L_{corr}}\right) \quad (6)$$

where d_{st} is the sampling distance and L_{corr} is the correlation distance. Note that shadowing is only applied to the coherent part [19]. $H_s(z)$ can slightly differ between the co- and cross-polar shadowing channels [1]. Thus, the filtering step can modify the correlation coefficient between two channels. To deal with this effect, \mathbf{R}_l can be weighted by a correction coefficient prior to taking its Cholesky factorization [17]. The correction coefficient is given by [17]

$$C_{correct} = \frac{1 - b_{co}c_{cross}}{\sqrt{1 - b_{co}^2} \sqrt{1 - c_{cross}^2}} \quad (7)$$

where b_{co} and c_{cross} are the filter coefficients for the co- and cross-polar channels as defined in (6). The outputs of the shadowing filter are first weighted by the total coherent component parameter, $\sigma_{l_i}(t)$, and then added to the attenuated direct signal, $q_i(t)$ (which are estimated using MST [3] and [4]). The time series are then converted to linear scale (i.e., to lognormal distributed time series) to obtain the large scale fading. The small and large scale fading processes of each

channel are summed and weighted by $v_i(t)$ (estimated from the physical-statistical tree model reported in [3] and [4]) to account for the signal fading caused by wind swaying. Finally, the Doppler shift of the direct signal component is accounted for by multiplying each channel by $\exp(j\phi_i)$, where ϕ_i is the phase corresponding to the traveled distance. The outputs of the simulator are partially correlated complex signal envelopes of the dual polarized 2×2 MIMO channel which incorporate the total fading caused by vegetation. Note that the model is also applicable in the nomadic case by assuming that wind swaying is the main cause of signal fading.

Fig. 12 shows examples of simulated partially correlated roadside tree LMS dual polarized MIMO channel time series. The system parameters used in the simulations are given in Table II. Sizes, densities and dielectric constants of tree components reported in [13, Table I] were used. The periodic fading in the time series of the co-polar components indicate the presence of trees along the road. As expected, the simulated cross-polar levels are lower than the co-polar components.

IV. PERFORMANCE EVALUATION

A. Channel capacity

For a narrowband MIMO system with N_t transmit and M_r receiver antennas, the receive signal is expressed as

$$\mathbf{r} = \mathbf{H}\mathbf{a} + \mathbf{n} \quad (8)$$

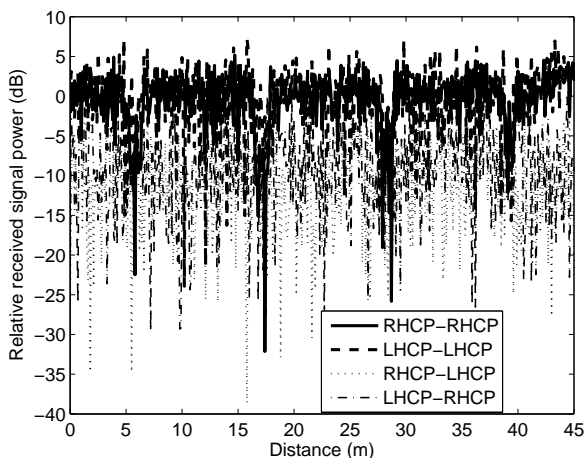


Fig. 12. Simulated partially correlated 2×2 dual polarized MIMO channel time series. Simulation parameters are given in Table II.

TABLE II
SYSTEM SIMULATION PARAMETERS

Type	Parameter	Value
System	Frequency	2 GHz
	Elevation angle	30°
	Azimuth angle	60°
	Speed of the mobile terminal	10 m/s
	Signal-to-noise ratio	20 dB
Tree	Canopy height	10 m
	Trunk height	10 m
	Canopy radius	5 m
	Trunk radius	0.4 m
	Number of trees in each side of the road	4
	Spacing between tree trunks	11 m
	Number of scatterers in a tree	100
	Width of the road	10 m
Wind	Mean wind speed	2 m/s

where \mathbf{a} is the transmitted signal, \mathbf{n} is the noise and \mathbf{H} is the $M_r \times N_t$ channel matrix with \mathbf{H}_{ij} being the channel response between the j th transmit antenna and the i th receive antenna. The capacity is given by [20]

$$C = \log_2 \left[\det \left(\mathbf{I}_{M_r} + \left(\frac{\bar{\gamma}}{N_t} \right) \mathbf{H}\mathbf{H}^H \right) \right] \text{ b/s/Hz} \quad (9)$$

where \mathbf{I}_{M_r} is the identity matrix of size M_r , $\bar{\gamma}$ is the average signal-to-noise ratio, \mathbf{H}^H is the complex transpose of the MIMO channel matrix, \mathbf{H} , and $\det(\cdot)$ denotes the matrix determinant. For the SISO case, the capacity is given by [20]

$$C = \log_2 \left(1 + \bar{\gamma} |h|^2 \right) \text{ b/s/Hz} \quad (10)$$

where h is the normalized complex channel gain relative to the LOS.

Fig. 13 presents the cumulative distribution functions (CDFs) of the LMS channel capacities for the dual polarized MIMO and SISO cases calculated using (9) and (10), respectively. The channel time series are generated using the simulator shown in Fig. 11 using the parameters listed in

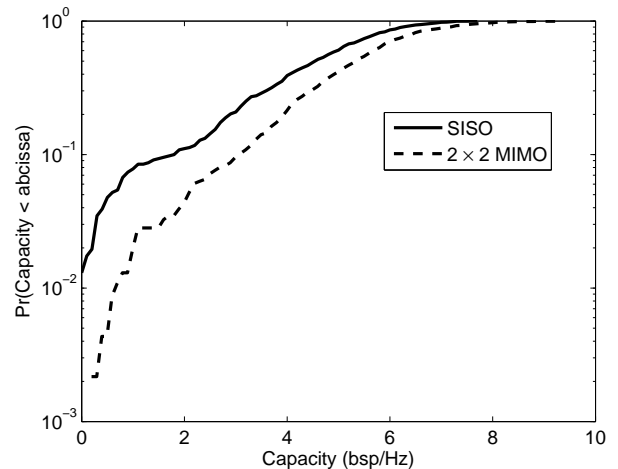


Fig. 13. CDFs of the LMS channel capacities along the roadside tree scenario simulated both for SISO and dual polarized MIMO cases. The system simulation parameters are given in Table II. A signal-to-noise ratio of 20 dB is used.

Table II. As expected, we can observe the increase in capacity achieved with MIMO compared to the SISO case.

B. Link diversity

Diversity improves link availability. The amount of diversity gain/improvement obtained depends on the degree of correlation between the various parallel links which, in turn, depends on the propagation environment. For the dual polarized MIMO case, the instantaneous signal-to-noise ratio at the output of the maximum-ratio-combiner (MRC) is given by [21]–[23]

$$\gamma = \bar{\gamma} \lambda_{\max} \quad (11)$$

where λ_{\max} is the largest eigenvalue of $\mathbf{H}\mathbf{H}^H$ for $N_t \geq M_r$ (or $\mathbf{H}^H\mathbf{H}$ for $N_t \leq M_r$). For SISO case

$$\gamma = \bar{\gamma} \left(|h_1|^2 + |h_2|^2 \right) \quad (12)$$

where h_1 and h_2 are the complex envelopes of the SISO channel.

Fig. 14 presents the CDFs of the received signal for the LMS roadside tree scenario for SISO, SIMO/space diversity (for two co-polar RHCP antennas, one wavelength apart) and dual polarized MIMO diversity with MRC. We can observe the significant diversity gain achieved with dual polarized MIMO and SIMO/space diversity compared to the SISO case. It can also be seen that the best performance is achieved with dual polarized MIMO diversity. This is because, firstly, the cross-polar components are not lost and contribute to increase the sum of signal-to-noise ratios at the output of the MRC. Secondly, we can observe from Fig. 12 that the cross-polar components are especially useful when the link is shadowed by the roadside trees. At these positions, the levels of the co- and cross-polar components are comparable (see Fig. 12) which results in significant diversity gains.

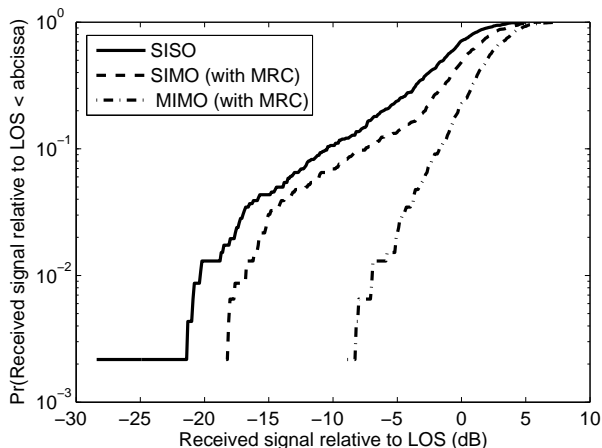


Fig. 14. CDFs of the LMS received signal along roadside tree areas for SISO, SIMO receiver space diversity (for two co-polar RHCP antennas, one wavelength apart) and dual polarized MIMO diversity links. The system simulation parameters are given in Table II.

V. CONCLUSION

In this paper we studied the LMS dual polarized MIMO channel along roadside tree areas. A novel physical-statistical, generative tree model based on multiple scattering theory was proposed for calculating the attenuation and scattering effects. FDTD electromagnetic computations were performed to characterize the tree scattering pattern and to calculate the shadowing cross-correlation matrix of the dual polarized MIMO channel. Generally, the use of FDTD has advantages in obtaining an accurate solution of electromagnetic interaction with arbitrary objects, however, it also has limitations in terms of the size of the computation volume relative to the wavelength, which is directly related to the required simulation time. This means that performing FDTD simulations over large computation areas/volumes may not be feasible, even using parallel computing.

In addition, a channel model/simulator for the SIMO receiver space diversity was also presented using the physical-statistical tree model, thus extending the SISO model in [3] and [4]. The physical-statistical approaches discussed are more effective for simulating large scenarios compared to complex physical models, and more accurate than merely empirical or statistical models.

In addition, performance analyses of the LMS SISO, dual polarized MIMO and SIMO/space diversity configurations were carried out. Compared to the SISO case, significant increases in performance were observed for the dual polarized MIMO and SIMO/space diversity cases. The results obtained can be used to evaluate the technical feasibility of LMS systems in roadside tree scenarios. They also give an insight into the kinds of system performance analyses which could be carried out using the models developed in this paper.

In general, the proposed channel models can be used to carry out different system-level analyses such as capacity, bit-error-rate, etc. Future work includes validating the developed LMS dual polarized MIMO and SIMO/space diversity channel models using measurements, as well as carrying out further

comparisons between MST and FDTD results.

ACKNOWLEDGMENT

The authors would like to thank the French Space Agency (CNES), French Aerospace Lab (ONERA) and Thales Alenia Space - France for supporting this work. The authors would also like to thank Xavier Ferrieres and Elodie Bachelier of ONERA for helping with the FDTD computations. In addition, the authors would like to thank Laurent Castanet of ONERA for his useful comments.

REFERENCES

- [1] P. R. King and S. Stavrou, "Low elevation wideband land mobile satellite MIMO channel characteristics," *IEEE Trans. Wireless Commun.*, vol. 6, no. 7, pp. 2712–2720, July 2007.
- [2] M. O. Al-Nuaimi and A. M. Hammoudeh, "Measurements and predictions of attenuation and scatter of microwave signals by trees," *IEE Proc. Microw. Ant. Prop.*, vol. 141, no. 2, pp. 70–76, April 1994.
- [3] M. Cheffena and F. P. Fontan, "Land mobile satellite channel simulator along roadside trees," *IEEE Ant. Wirel. Prop. Letters*, vol. 9, pp. 748–751, 2010.
- [4] —, "Channel simulator for land mobile satellite channel along roadside trees," *IEEE Trans. Ant. Prop.*, vol. 59, no. 5, pp. 1699–1706, May 2011.
- [5] G. J. Byers and F. Takawira, "Spatially and temporally correlated MIMO channels: Modeling and capacity analysis," *IEEE Trans. Veh. Techn.*, vol. 53, no. 3, pp. 634–643, May 2004.
- [6] C. Oestges, "A stochastic geometrical vector model of macro- and megacellular communication channels," *IEEE Trans. Veh. Techn.*, vol. 51, no. 6, pp. 1352–1360, November 2002.
- [7] M. Sellathurai, P. Guinand, and J. Lodge, "Space-time coding in mobile satellite communications using dual-polarized channels," *IEEE Trans. Veh. Techn.*, vol. 55, no. 2, pp. 188–199, January 2006.
- [8] G. Alfano and A. D. Maio, "A theoretical framework for LMS MIMO communication systems performance analysis," *In proc. 3rd Int. Waveform Diversity and Design Conf.*, June 2007.
- [9] K. P. Liolis, J. Gomez-Vilardebo, E. Casini, and A. Perez-Neira, "On the statistical modelling of MIMO land mobile satellite channels: A consolidated approach," *27th AIAA Int. Commu. Sat. Sys. Conf. (ICSSC)*, Edinburgh, June 2009.
- [10] L. L. Foldy, "The multiple scattering of waves," *Phys. Rev.*, vol. 67, no. 3, pp. 107–119, 1945.
- [11] M. X. Lax, "Multiple scattering of waves," *Rev. Mod. Phys.*, vol. 23, no. 4, pp. 287–310, 1951.
- [12] S. A. Torricco, H. L. Bertoni, and R. H. Lang, "Modeling tree effects on path loss in a residential environment," *IEEE Trans. Ant. Prop.*, vol. 46, no. 6, pp. 872–880, June 1998.
- [13] Y. L. C. de Jong and M. H. A. J. Herben, "A tree-scattering model for improved propagation prediction in urban microcells," *IEEE Trans. Veh. Techn.*, vol. 53, no. 2, pp. 503–513, March 2004.
- [14] K. S. Yee, "Numerical solution of initial boundary value problems involving Maxwells equations in isotropic media," *IEEE Trans. Ant. Prop.*, vol. AP-14, no. 3, pp. 302–307, May 1966.
- [15] A. A. Chukhlantsev, A. M. Shutko, and S. P. Golovachev, "Conductivity of leaves and branches and its relation to the spectral dependence of attenuation by forests in meter and decimeter band," *In Proc. IEEE Int. Geosci. and Remote Sensing Sym.*, pp. 1103–1105, 21–25 July 2003.
- [16] N. C. Rogers, A. Seville, J. Richter, D. Ndzi, N. Savage, R. Caldeirinha, A. K. Shukla, M. Al-Nuaimi, K. Craig, E. Vilar, and J. Austin, "A generic model of 1-60 GHz radio propagation through vegetation - Final report," Radio Agency, UK, May 2002.
- [17] G. Carrie, J. Lemorton, and F. Perez-Fontan, "State-of-the-art review of LMS MIMO channel models at S and C band upgrade of the validity domain of the available channel models," Technical report, ONERA, April 2010.
- [18] T. Aulin, "A modified model for the fading signal at a mobile radio channel," *IEEE Trans. Veh. Techn.*, vol. 28, no. 3, pp. 182–203, August 1979.
- [19] F. Perez-Fontan and P. M. Espineira, *Modelling the Wireless Propagation Channel: A Simulation Approach with MATLAB*. John Wiley and Sons Ltd., Chichester, UK, ISBN: 978-0-470-72785-0, 2008.

- [20] J. G. Foschini and J. M. Gans, "On limits of wireless communications in a fading environment when using multiple antennas," *Wire. Pres. Commun.*, pp. 311–335, 6, (3), 1998.
- [21] T. K. Y. Lo, "Maximum ratio transmission," *IEEE Trans. Commun.*, vol. 47, pp. 1458–1461, 1999.
- [22] C. H. Tse, K. W. Yip, and T. S. Ng, "Performance tradeoffs between maximum ratio transmission and switched-transmit diversity," in *Proc. 11th IEEE Int. Symp. Personal, Indoor, Mobile Radio Commun.*, pp. 1485–1489, 2000.
- [23] M. Kang and M. S. Alouini, "Largest egevalue of complex wishart matrices and performance analysis of MIMO MRC systems," *IEEE J. Select. Commun.*, vol. 21, no. 3, pp. 418–431, April 2003.